Alkenone unsaturation in surface sediments from the eastern equatorial Pacific: Implications for SST reconstructions

M. Kienast,[1] G. MacIntyre,[1] N. Dubois,[1,3] S. Higginson,[1] C. Normandeau,[1] C. Chazen,[2] and T. D. Herbert[2]

Received 4 November 2011; revised 17 January 2012; accepted 18 January 2012; published 14 March 2012.

[1] Significant uncertainties persist in the reconstruction of past sea surface temperatures in the eastern equatorial Pacific, especially regarding the amplitude of the glacial cooling and the details of the post-glacial warming. Here we present the first regional calibration of alkenone unsaturation in surface sediments versus mean annual sea surface temperatures (maSST). Based on 81 new and 48 previously published data points, it is shown that open ocean samples conform to established global regressions of $U^{K'}_{37}$ versus maSST and that there is no systematic bias from seasonality in the production or export of alkenones, or from surface ocean nutrient concentrations or salinity. The flattening of the regression at the highest maSSTs is found to be statistically insignificant. For the near-coastal Peru upwelling zone between 11–15°S and 76–79°W, however, we corroborate earlier observations that $U^{K'}_{37}$ SST estimates significantly over-estimate maSSTs at many sites. We posit that this is caused either by uncertainties in the determination of maSSTs in this highly dynamic environment, or by biasing of the alkenone paleothermometer toward El Niño events as postulated by Rein et al. (2005).

Citation: Kienast, M., G. MacIntyre, N. Dubois, S. Higginson, C. Normandeau, C. Chazen, and T. D. Herbert (2012), Alkenone unsaturation in surface sediments from the eastern equatorial Pacific: Implications for SST reconstructions, *Paleoceanography*, *27*, PA1210, doi:10.1029/2011PA002254.

1. Introduction

[2] The eastern equatorial Pacific (EEP) is arguably the oceanic region where reconstructions of past sea surface temperature (SST) variability based on different proxies disagree most significantly. For instance, foraminiferal Mg/Ca and alkenone paleothermometry-based SST estimates disagree on the timing and pattern of the glacial-interglacial warming [*Kienast et al.*, 2006; *Lea et al.*, 2006; *Prahl et al.*, 2006], and the inferred amplitude of the glacial cooling, in particular in the cold tongue off Peru, ranges from 2 to 8°C depending on the proxy used [*Dubois et al.*, 2009; *Feldberg and Mix*, 2002, 2003; *Koutavas and Lynch-Stieglitz*, 2003; *Mix et al.*, 1999; *Pisias and Mix*, 1997; *Rein et al.*, 2005]. In turn, the gradient in SSTs between this cold tongue and the warm pool to the north is thus postulated to have been either stronger or weaker during the Last Glacial Maximum (LGM) compared to the Holocene [*Dubois et al.*, 2009; *Koutavas and Lynch-Stieglitz*, 2003]. According to records of alkenone unsaturation, the EEP was consistently warmer during the late Holocene compared to the early Holocene, whereas foraminiferal Mg/Ca records suggest a regionally diverse and variable change in SSTs during the last 10,000 years [*Leduc et al.*, 2010]. Overall, the ambiguity in SST reconstructions severely limits our understanding of fundamental aspects and processes in this climatically important area, and ultimately hinders quantitative assessment of climate repercussions globally.

[3] Studies of algal cultures, water column particulates and sediment samples, respectively, have shown that the relative proportion of di-(C37:2) and tri-(C37:3) unsaturated alkenones, expressed as the $U^{K'}_{37}$ index [C37:2/(C37:2 + C37:3)], varies with growth temperature of the algae [*Prahl and Wakeham*, 1987]. Despite the strong variability of environmental and ecological conditions throughout the global ocean, the $U^{K'}_{37}$ index has provided oceanographers with a remarkably reliable tool to estimate past SSTs from alkenones preserved in the sedimentary record. The most commonly used calibration of $U^{K'}_{37}$ versus mean annual sea surface temperatures (maSST) was initially derived from phytoplankton cultures by *Prahl et al.* [1988] and later validated and refined by global sedimentary calibrations by *Müller et al.* [1998] and *Conte et al.* [2006]. It has proven valid over a large range of SSTs, with an approximate standard error of estimate of 0.05 $U^{K'}_{37}$ units, equivalent to 1.5°C [*Müller et al.*, 1998].

[4] While the calibration of *Müller et al.* [1998] has provided a robust proxy for maSST between 0 and 29°C, it has been suggested that the temperature dependence of the unsaturation index may weaken at both the warm and cold end of the calibration. In efforts to improve the calibration at

[1]Department of Oceanography, Dalhousie University, Halifax, Nova Scotia, Canada.
[2]Department of Geological Sciences, Brown University, Providence, Rhode Island, USA.
[3]Now at School of Earth, Atmospheric and Environmental Sciences, University of Manchester, Manchester, UK.

0883-8305/12/2011PA002254

the warm end, *Sonzogni et al.* [1997] offered a regional linear calibration derived from surface sediments in the Indian Ocean for surface temperatures ranging from 24 to 30°C. The calibration presented for this temperature range suggests that there is a 35% decrease in the slope at the warm end relative to global calibrations. Alternatively, *Conte et al.* [2006] developed a nonlinear, global core top calibration to account for the 'warm-end' bias. Studies of $U^{K'}_{37}$ in surface sediments from the equatorial Atlantic [*Müller and Fischer*, 2003; *Schneider et al.*, 1995] and the South China Sea [*Pelejero and Grimalt*, 1997], on the other hand, do not reveal a decrease in sensitivity at the warm end (note that in contrast to *Müller and Fischer* [2003] and *Schneider et al.* [1995], *Müller et al.* [1998] state that "there seems to be some systematic flattening" at the warm end in the extended tropical Atlantic data set presented in the latter study).

[5] Another uncertainty in alkenone paleothermometry is related to seasonality. Because of the obvious and globally non-uniform seasonality in the production and flux to the seafloor of alkenones, it is counter intuitive to expect alkenone unsaturation to reflect annual average temperatures throughout the world's ocean. While *Müller et al.* [1998] conclude that "seasonal changes in primary production have only a negligible effect on the $U^{K'}_{37}$ signal," a number of studies suggest that there is indeed a seasonal aliasing of the SST signal recorded in alkenones [*Prahl et al.*, 2010; *Schneider et al.*, 2010]. In addition, discrepancies between SST estimates based on down-core records of alkenone unsaturation and foraminiferal Mg/Ca and $\delta^{18}O$, respectively, have been interpreted to reflect seasonal differences in the production of the signal carriers [e.g., *Haug et al.*, 2005; *Steinke et al.*, 2008]. Most recently, *Prahl et al.* [2010] reported that "significant biogeographical patterns seem apparent" in the $U^{K'}_{37}$-temperature residuals along the west coast of the Americas and in the North Atlantic. Specifically, these authors argued that the observed warm mismatch between alkenone-based SST estimates and SSTs from the World Ocean Atlas (WOA) is consistent with an "export production dominance in summer when surface waters are warmest, [and] nutrients least available." This inference is in line with observations that coccolithophores thrive under low nutrient conditions in quiescent waters, i.e., during non-upwelling conditions [*Aksnes et al.*, 1994; *Tyrrell and Merico*, 2004], but conflicts with the observed coincidence of warm waters and maximum productivity off Peru [*Pennington et al.*, 2006; *Gutiérrez et al.*, 2011]. Similarly, *Rein et al.* [2005] suggested that coccolithophores off Peru reach their maximum abundance during El Niño warm water anomalies, thus skewing the alkenone paleothermometer toward warm water conditions. More generally, laboratory cultures have suggested that non-thermal factors, such as nutrient stress, can contribute to variability in alkenone unsaturation [e.g., *Prahl et al.*, 2003], and *Prahl et al.* [2006] posit that such physiological factors indeed affect $U^{K'}_{37}$ values in the EEP, possibly skewing reconstructions of past SSTs. These authors also suggested that such physiological effects alter the overall alkenone/alkenoate biosynthesis, as reflected in the compositional indices %K37, %K38 and ME/K37. These indices quantify the percent distribution of C37 or C38 alkenones, respectively, relative to the total abundance of alkenones with C37–C39, and the proportion of C36 methyl ester to total C37 alkenones.

[6] The EEP is an ideal test bed to explore possible biases of alkenone paleothermometry because it is a tropical ('warm end') ocean region with large gradients in SSTs and nutrient conditions, and regionally restricted strong seasonality (see below). Here we present 81 new $U^{K'}_{37}$ data from surface sediments in the EEP, and combine them with 48 previously published data points to arrive at a regional picture of alkenone unsaturation. Specifically, we will use these data to assess the extent to which $U^{K'}_{37}$-based SST reconstructions appear to be biased by the seasonality and/or 'warm end' bias, or by other factors that have been postulated to affect alkenone unsaturation such as nutrient availability or salinity. In a final chapter we explore paleoceanographic implications of our findings in light of the contradictory reconstructions of past SSTs in the EEP summarized above.

2. Study Region

[7] The EEP is characterized by strong climatic asymmetries. The region north of the equator hosts a warm pool and intense rainfall due to the overlying Intertropical Convergence Zone (ITCZ) [*Mitchell and Wallace*, 1992; *Li and Philander*, 1996; *Xie et al.*, 2005]. Year-round southeasterly trade winds blowing across the equator and into the ITCZ create a tongue of cold water centered at 1°S in the South Equatorial Current (SEC): the Equatorial Upwelling (EU). Horizontal advection in the Peru Current of cool water upwelled along the coast of Peru contributes to this cold tongue which extends westward to 130°W [*Wyrtki*, 1981]. Beneath the SEC lies the Equatorial Undercurrent, which flows eastward across the Pacific at depths of 200–250 m. The upper portion of this current is the source of the water upwelled along the equator [*Wyrtki*, 1981], whereas the lower portion of the current continues eastward as the Peru Undercurrent, upwelling off the coast of Peru [*Toggweiler et al.*, 1991]. In the Peruvian Coastal Upwelling (PCU), upwelling proceeds almost year-round because of persistent alongshore winds producing seaward Ekman transport of surface water [*Chavez*, 1995]. In contrast, the EU intensifies during boreal summer, when the ITCZ is in its northernmost position. The cold tongue diminishes or vanishes during boreal winter, when the ITCZ is in its southernmost position [*Li and Philander*, 1996].

[8] As a consequence of the EEP's complex hydrography and atmospheric forcing, distinct biogeographic regions coexist (Equatorial Upwelling, Eastern margin and open ocean regions [see *Pennington et al.*, 2006]). Spatial patterns of primary production reveal zones of high productivity along the coast of Peru, the equator, west of the Galápagos Islands and in the central American Gulfs, again with significant north–south asymmetries [*Pennington et al.*, 2006]. The southern hemisphere PCU region has by far the highest chlorophyll concentrations, and this biomass extends to 1000 km offshore. In contrast, the Gulfs of Panama, Papagayo and Tehuantepec are impressive in satellite images of chlorophyll, but ship-collected data suggest chlorophyll concentrations considerably lower than observed with SeaWiFS [*Pennington et al.*, 2006].

[9] Though primary production is significantly higher in the EU than in other open-ocean regions, its phytoplankton assemblage is dominated by small solitary cells characteristic of the subtropical gyres [*Chavez*, 1989; *Chavez et al.*, 1991,

1996; *Landry and Kirchman*, 2002]. The EU exhibits a weak seasonality of surface chlorophyll, with a maximum during boreal summer, the season of strongest upwelling.

[10] PCU region phytoplankton on the other hand exhibit strong seasonality, with the highest levels of chlorophyll and primary production occurring during the austral summer and fall [*Chavez*, 1995]. This seasonal cycle is perplexing given that the maximum coastal upwelling occurs from June through November [*Scheidegger and Krissek*, 1981] because of maximum southeast trade wind intensities [*Bakun*, 1987; *Bakun and Nelson*, 1991]. This out-of-phase seasonality of upwelling and chlorophyll has been attributed to iron and light limitation of productivity in winter, as well as vertical dilution of the biomass in winter by a deepening of the mixed layer depth [*Chavez et al.*, 2008; *Echevin et al.*, 2008; *Friederich et al.*, 2008].

[11] PCU chlorophyll concentrations are maximum nearshore and decrease gradually offshore. The nearshore area between 6°S and 15°S is characterized by extensive diatom blooms and has thus been referred to as the "brown waters of Peru" by *Strickland et al.* [1969]. These diatom blooms and the high rates of macronutrient assimilation are sustained by an adequate external supply of iron [*Bruland et al.*, 2005], which is provided by the suboxic conditions of the Peru Undercurrent waters in contact with organic rich shelf sediments [*Morales et al.*, 1999; *Hutchins et al.*, 2002]. In contrast, the southern coastal upwelling and offshore regions of the Peru Current lack this external supply of iron and the waters evolve into Fe-limited HNLC "blue waters" containing relatively low diatom biomass and Chl a [*Minas and Minas*, 1992; *Bruland et al.*, 2005]. "Blue water" phytoplankton communities are dominated by haptophytes [*Hutchins et al.*, 2002], whereas large diatoms are the most abundant phytoplankton group inhabiting the coastal upwelling "brown waters" [*Rojas de Mendiola*, 1981; *Wilkerson et al.*, 2000; *Iriarte and Gonzalez*, 2004; *DiTullio et al.*, 2005].

[12] Interannual to multidecadal phenomena (El Niño, El Viejo) deepen the eastern Pacific thermocline and nutricline, resulting in dramatic fluctuations in ecosystem productivity [*Barber and Chavez*, 1983, 1986]. During these events, upwelling is fed with warm and nutrient depleted surface waters and cannot reach into the cooler and nutrient-rich deeper waters [*Rein et al.*, 2005]. The modified chemistry of upwelled water results in a substantial decrease in surface productivity along with warm surface water anomalies [*Arntz and Fahrbach*, 1991]. The strongest impacts of El Niños and El Viejos are felt in the EU and PCU regions [*Fiedler*, 2002]. In the PCU, the phytoplankton community shifts from diatoms and larger phytoplankton to a community of picoplankton more typical of the open-ocean (cyanobacteria and prochlorophytes) [*Chavez*, 2005]. Coccolithophoridae, which preferentially grow during the months with warmer SST and less nutrient availability, reach their maximum abundance in the PCU during the El Niño warm water anomalies when surface water is depleted in nutrients [*Rein et al.*, 2005].

3. Methods and Materials

[13] For the purpose of this study, the EEP is defined as the ocean region between 20°N and 20°S, east of 125°W and west of the central and South American coast. Forty eight of the samples in this study are taken from the top 1 cm of multicores recovered during recent expeditions of the R/V *Melville* (ME0005A in 2000) and R/V *Knorr* (176–2 in 2002, 182–9 in 2005, and 195–5 in 2009). In addition, we received samples from a number of core repositories (see acknowledgments for details). The data compilation presented here also includes core tops from previous studies (see Table 1). While we can ascertain that the former samples are true surface sediments, the tops of piston and gravity cores may not. Note, however, that the paucity of radiocarbon ages does not allow the unambiguous assignment of "modern" to even the best of surface sample. However, none of the observations presented below depends exclusively on either one of the different sample sets.

[14] All samples were analyzed according to well-established analytical protocols [e.g., *Kienast et al.*, 2006; *Dubois et al.*, 2009]. Briefly, a Dionex Accelerated Solvent Extraction system (ASE200) was used to extract total lipids from 1 to 2 g of freeze-dried sediment with DCM:MeOH, 93:7 v:v. The extracts were saponified using potassium hydroxide and purified through silica column chromatography. The purified extracts were analyzed by gas chromatography. Based on replicate analysis and repeat extractions, the analytical precision of the method is 0.01 $U^{K'}_{37}$ units, equivalent to ca. 0.3°C according to the calibration of *Prahl et al.* [1988]. For selected samples (n = 18), the detailed alkenone/alkenoate signature [*Brassell*, 1993] was also determined. Thus, %K37, %K38, ME/K37 were quantified based on the gas chromatographic retention time of the C36 methyl ester (ME) and all C37, C38 and C39 carbon-chain-length alkenones, as identified by analogy to the retention time of these compounds in the chromatogram of an extract of an *E. huxleyi* culture sample.

[15] Since this study combines data from different laboratories, analytical offsets between laboratories are a possible concern. According to an inter-laboratory comparison by *Rosell-Melé et al.* [2001], the maximum difference between any two laboratories is <2.1°C. However, two lines of evidence suggest that this is a pessimistic estimate with respect to the data presented here. (1) Downcore $U^{K'}_{37}$ SST records analyzed at Dalhousie University (TR163–31 [*Dubois et al.*, 2011] and ME0005A-43 (N. Dubois et al., unpublished data, 2010)) agree to within 0.3–0.8°C with $U^{K'}_{37}$ SST records from closely adjacent sites (V19–30 [*Koutavas and Sachs*, 2008] and MD02–2529 [*Leduc et al.*, 2007]) determined in other laboratories. (2) Specifically for the present study, the $U^{K'}_{37}$ in seven surface sediment samples from the EEP, previously analyzed by *Kusch et al.* [2010] (n = 1), *Pahnke et al.* [2007] (n = 2) and at Brown University (n = 4; this study), was determined. The differences between the Dalhousie $U^{K'}_{37}$ and the other three laboratories range from −0.019 to 0.026, with an average of 0.005. It thus appears that the substantial discrepancy between closely adjacent sites ME0005A-24JC and Y69–71 [*Kienast et al.*, 2006; *Prahl et al.*, 2006] is an anomaly, which is the subject of an ongoing investigation (F. Prahl and M. Kienast, unpublished data, 2010). Note, however, that none of the conclusions below is based on the results from a single laboratory.

[16] Present-day mean annual and seasonal SST data, mean annual surface ocean phosphate concentrations and

Table 1. $U^{K'}_{37}$ and Ancillary Data for EEP Surface Sediments

Core ID	Latitude	Longitude (°W)	$U^{K'}_{37}$	maSST (WOA09)	Prahl SST	Residual	Reference
RR9702A-62MC1	−18.1	79.0	0.698	19.96	19.38	−0.58	*Prahl et al.* [2006]
RR9702A-64MC1	−17.0	78.1	0.701	20.01	19.47	−0.54	*Prahl et al.* [2006]
RR9702A-70MC1	−16.7	76.0	0.661	19.68	18.29	−1.38	*Prahl et al.* [2006]
RR9702A-72MC1	−16.5	76.2	0.696	19.68	19.32	−0.36	*Prahl et al.* [2006]
RR9702A-74MC1	−16.2	76.2	0.675	19.68	18.71	−0.97	*Prahl et al.* [2006]
RR9702A-77MC1	−16.1	77.0	0.677	19.82	18.76	−1.06	*Prahl et al.* [2006]
RR9702A-66MC1	−16.1	77.1	0.677	19.82	18.76	−1.06	*Prahl et al.* [2006]
RR9702A-68MC1	−16.0	76.4	0.685	19.68	19.00	−0.68	*Prahl et al.* [2006]
RR9702A-82MC4	−13.7	76.7	0.736	19.13	20.50	1.37	*Prahl et al.* [2006]
RR9702A-80MC4	−13.5	76.9	0.699	19.13	19.41	0.28	*Prahl et al.* [2006]
RR9702A-83MC2	−13.2	77.3	0.748	19.13	20.85	1.72	*Prahl et al.* [2006]
VNTR01-10GC	−4.5	102.0	0.867	24.29	24.35	0.06	*Prahl et al.* [2006]
VNTR01-9PC	−3.0	110.5	0.876	24.52	24.62	0.10	*Prahl et al.* [2006]
VNTR01-12GC	−3.0	95.1	0.802	23.52	22.44	−1.08	*Prahl et al.* [2006]
VNTR01-8PC	0.0	110.5	0.868	24.30	24.38	0.08	*Prahl et al.* [2006]
VNTR01-19PC	7.9	90.5	0.911	27.32	25.65	−1.67	*Prahl et al.* [2006]
VNTR01-21GC	9.6	94.6	0.908	27.76	25.56	−2.20	*Prahl et al.* [2006]
MWSC2	−11.1	78.1	0.777	20.35	21.71	1.35	*Conte et al.* [2006]
Peru3MC1	−12.7	77.6	0.746	19.00	20.79	1.80	*Conte et al.* [2006]
Peru2MC4	−12.5	77.6	0.647	19.00	17.88	−1.11	*Conte et al.* [2006]
Peru4MC2	−12.5	77.5	0.762	19.00	21.26	2.27	*Conte et al.* [2006]
Peru1MC3	−12.4	77.5	0.747	19.00	20.82	1.83	*Conte et al.* [2006]
Peru Upwelling	−12.0	77.3	0.550	19.00	15.03	−3.97	*Conte et al.* [2006]
SC3	−15.1	75.7	0.710	19.24	19.74	0.49	*Conte et al.* [2006]
MWSC7	−14.9	75.6	0.656	18.32	18.15	−0.17	*Conte et al.* [2006]
PLDS66	1.0	124.5	0.826	25.90	23.13	−2.76	*Conte et al.* [2006]
PLDS_90, 5–10	1.1	119.9	0.938	25.08	26.44	1.36	*Conte et al.* [2006]
PLDS74, 5–10	1.0	113.7	0.895	24.77	25.16	0.39	*Conte et al.* [2006]
PLDS_68, 5–10	1.1	107.2	0.885	24.77	24.88	0.11	*Conte et al.* [2006]
PLDS72, 5–10	1.1	107.2	0.888	24.77	24.96	0.19	*Conte et al.* [2006]
PLDS_70, 5–10	1.0	105.5	0.886	24.76	24.90	0.14	*Conte et al.* [2006]
PLDS_70, 5–10	0.9	104.1	0.873	24.20	24.53	0.33	*Conte et al.* [2006]
PLDS_77, 5–10	1.0	104.1	0.914	24.20	25.72	1.52	*Conte et al.* [2006]
V19-27	−0.3	82.4	0.941	24.52	26.54	2.03	*Koutavas and Sachs* [2008]
V19-28	−2.2	84.4	0.856	22.85	24.04	1.18	*Koutavas and Sachs* [2008]
V19-30	−3.2	83.3	0.812	22.12	22.73	0.61	*Koutavas and Sachs* [2008]
V21-30	−1.1	89.4	0.881	23.41	24.76	1.36	*Koutavas and Sachs* [2008]
RC11-238	−1.3	85.5	0.870	23.49	24.43	0.94	*Koutavas and Sachs* [2008]
HY06	0.0	95.3	0.855	24.35	24.00	−0.34	*Horikawa et al.* [2006]
Y69-71P	0.1	86.5	0.857	25.00	24.06	−0.94	*Prahl et al.* [2006]
MD02-2529	8.1	84.1	0.954	28.49	26.91	−1.58	*Leduc et al.* [2007]
ODP-846	−3.1	90.5	0.803	23.33	22.47	−0.86	*Liu and Herbert* [2004]
TR163-19	2.2	90.6	0.893	26.33	25.12	−1.22	*Dubois et al.* [2009]
TR163-22	0.3	92.2	0.858	24.15	24.10	−0.05	*Dubois et al.* [2009]
TR163-31	−3.4	83.6	0.792	22.12	22.13	0.02	*Dubois et al.* [2009]
TG7 (MC)	−17.2	78.6	0.730	20.01	20.32	0.31	*Calvo et al.* [2001]
SO147-106KL	−12.0	77.4	0.763	19.00	21.30	2.30	*Rein et al.* [2005]
B0406	−14.1	76.3	0.647	18.32	17.88	−0.44	*Gutiérrez et al.* [2011]
AMPH-25G	−9.1	105.9	0.911	24.82	25.64	0.81	this study
CARR12	−8.9	103.5	0.894	24.76	25.14	0.38	this study
DWBG-143	−3.6	114.3	0.895	24.80	25.17	0.37	this study
DWBG-144	−1.2	115.8	0.920	24.27	25.91	1.63	this study
GS7202-20	−8.8	98.0	0.924	24.37	26.03	1.67	this study
GS7202-19	−7.0	98.0	0.930	24.35	26.20	1.85	this study
GS7202-23	−8.4	101.5	0.922	24.62	25.97	1.35	this study
GS7202-24	−10.0	101.6	0.911	24.48	25.65	1.17	this study
GS7202-40	−18.0	102.6	0.901	23.03	25.34	2.31	this study
GS7202-46	−12.3	78.5	0.893	19.97	25.12	5.15	this study
GS7202-52	−12.8	79.5	0.905	20.58	25.46	4.88	this study
ME005A-04MC6	15.7	95.3	0.981	27.73	27.71	−0.03	this study
ME005A-07MC3	15.7	95.3	0.991	27.73	27.99	0.26	this study
ME005A-08MC4	15.6	95.3	0.941	27.73	26.54	−1.20	this study
ME005A-14MC7	5.8	86.4	0.976	27.63	27.56	−0.06	this study
ME005A-15MC6	4.6	86.7	0.946	27.41	26.68	−0.72	this study
ME005A-21MC4	0.0	86.5	0.915	25.00	25.76	0.77	this study
ME005A-25MC2	−1.9	82.8	0.845	23.52	23.70	0.18	this study
ME005A-29MC2	−0.5	82.0	0.921	24.91	25.95	1.04	this study
ME005A-35MC3	4.1	85.0	0.952	27.44	26.86	−0.58	this study
ME005A-38MC2	7.3	84.1	0.957	28.21	27.00	−1.21	this study
ME005A-41MC2	7.9	83.6	0.962	28.35	27.15	−1.20	this study
ME005A-20MC8	3.2	86.5	0.952	27.04	26.84	−0.20	this study

Table 1. (continued)

Core ID	Latitude	Longitude (°W)	$U^{K'}_{37}$	maSST (WOA09)	Prahl SST	Residual	Reference
P6702-G11	−5.0	103.0	0.897	24.56	25.23	0.67	this study
P6702-G13	−6.1	81.6	0.815	20.46	22.84	2.38	this study
P6702-G34	−9.3	109.9	0.917	25.11	25.81	0.71	this study
P6702-G52	−1.7	90.6	0.894	23.06	25.14	2.08	this study
P6702-G59	2.8	85.3	0.948	26.53	26.73	0.20	this study
RC13-106	−5.4	88.8	0.877	23.48	24.64	1.16	this study
RC13-108	−3.1	89.4	0.859	23.31	24.13	0.82	this study
RC13-142	4.5	82.4	0.963	27.22	27.17	−0.05	this study
RC18-46	−5.4	87.3	0.868	23.30	24.38	1.08	this study
RC18-48	−3.6	82.4	0.928	21.67	26.16	4.49	this study
RC23-20	1.0	83.6	0.920	25.90	25.92	0.03	this study
SCAN-95G	−5.0	114.1	0.890	25.33	25.03	−0.30	this study
KNR-176-2-MC11-D	5.3	77.4	0.972	26.68	27.44	0.76	this study
KNR-176-2-MC28-G	2.5	79.1	0.951	26.63	26.82	0.19	this study
KNR-176-2-MC4-A	7.2	78.1	0.949	28.33	26.78	−1.55	this study
KNR-176-2-MC24-F	3.5	78.1	0.956	26.77	26.96	0.19	this study
KNR-176-2-MC33-F	4.4	77.6	0.954	26.72	26.91	0.20	this study
KNR-176-2-MC7-G	6.5	77.6	0.953	26.63	26.89	0.26	this study
KNR-176-2-MC40-H	7.1	80.3	0.957	28.33	26.99	−1.34	this study
KNR-176-2-MC37-H	6.4	77.5	0.949	26.63	26.78	0.15	this study
KNR-176-2-MC14-G	4.5	77.4	0.959	26.72	27.05	0.34	this study
KNR-176-2-MC21-F	4.2	77.4	0.921	26.72	25.95	−0.77	this study
KNR-176-2-MC5-F	7.1	78.0	0.959	28.33	27.06	−1.26	this study
KNR182-9-MC2-E	−16.8	72.7	0.667	19.72	18.47	−1.26	this study
KNR182-9-MC3-A	−15.6	75.1	0.751	19.24	20.95	1.71	this study
KNR182-9-MC4-F	−13.3	77.2	0.782	19.13	21.85	2.72	this study
KNR182-9-MC6-E	−13.3	76.5	0.754	19.13	21.03	1.91	this study
KNR182-9-MC7-H	−12.8	77.0	0.800	19.00	22.39	3.40	this study
KNR182-9-MC8-C	−12.3	78.0	0.802	19.00	22.46	3.46	this study
KNR182-9-MC9-G	−11.7	78.4	0.800	20.35	22.37	2.02	this study
KNR182-9-MC10-F	−11.7	77.6	0.747	20.35	20.83	0.48	this study
KNR182-9-MC12-H	−11.0	78.2	0.822	20.35	23.02	2.67	this study
KNR182-9-MC13-E	−11.0	78.2	0.797	20.35	22.30	1.95	this study
KNR182-9-MC14-F	−8.2	80.3	0.774	20.35	21.62	1.27	this study
KNR182-9-MC15-F	−3.6	83.9	0.797	22.12	22.29	0.17	this study
KNR182-9-MC16-F	1.5	86.2	0.903	25.80	25.42	−0.39	this study
KNR182-9-MC17-H	8.5	90.0	0.937	27.30	26.41	−0.89	this study
KNR195-5-MC11-E	−1.3	86.5	0.840	23.53	23.56	0.02	this study
KNR195-5-MC33-E	−3.1	82.5	0.781	21.67	21.82	0.16	this study
KNR195-5-MC9-E	−0.5	87.5	0.849	24.17	23.82	−0.34	this study
KNR195-5-MC34-E	−3.4	83.6	0.788	22.12	22.03	−0.09	this study
KNR195-5-MC25-E	−3.3	81.0	0.777	21.29	21.71	0.42	this study
KNR195-5-MC42-D	−1.2	89.4	0.862	23.41	24.21	0.80	this study
KNR195-5-MC12-E	−3.4	81.1	0.819	21.29	22.94	1.66	this study
KNR195-5-MC38-E	−1.2	89.4	0.829	23.41	23.24	−0.17	this study
KNR195-5-MC16-E	−3.5	81.1	0.807	21.29	22.59	1.30	this study
KNR195-5-MC22-E	−3.5	81.2	0.823	21.29	23.06	1.77	this study
KNR195-5-MC18-E	−3.6	81.2	0.818	21.29	22.91	1.63	this study
ODP 1228	−11.1	78.1	0.791	20.35	22.11	1.76	this study
W7706-40K	−11.3	78.0	0.767	20.35	21.40	1.05	this study
GC-10	−14.9	75.6	0.721	18.32	20.05	1.73	this study
54-2-PG9	−8.1	104.3	1.000	25.08			this study
AMPH-19G	−8.3	107.8	1.000	25.40			this study
DWBG-140G	−5.9	112.5	1.000	25.51			this study
GS7202-022	−7.6	104.0	1.000	25.08			this study
GS7202-18	−6.9	97.9	1.000	24.52			this study
GS7202-38	−16.2	107.6	1.000	24.16			this study
P6702-G4	0.0	103.1	1.000	23.82			this study

salinity were taken from the World Ocean Atlas 2009 (WOA09) at one-degree resolution [*Locarnini et al.*, 2010; *Garcia et al.*, 2010; *Antonov et al.*, 2010]. Seasonality is calculated as WOA SSTs for July–September minus WOA SSTs for January–March. Correlation coefficients and linear regressions were computed using standard statistical techniques. Confidence intervals on the regression coefficients were calculated at the 95% level.

4. Results and Discussion

4.1. $U^{K'}_{37}$ in EEP Surface Sediments

[17] $U^{K'}_{37}$ values in the EEP range from 0.550 to 0.991 (Figures 1 and 2b and Table 1), with highest values

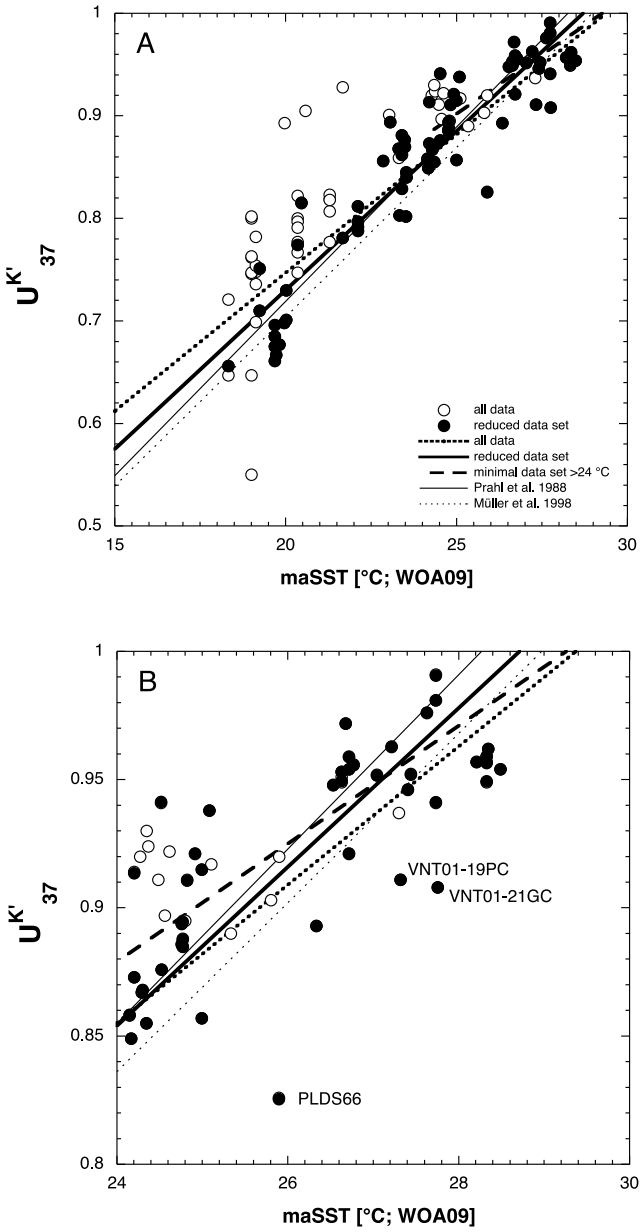

Figure 1. (a) Scatterplot of $U^{K'}_{37}$ indices in EEP surface sediments versus (WOA09) mean annual sea surface temperatures (maSST). Lines represent the best linear fit for the full (thick dotted line; all data points) and the reduced data sets (thick solid line, filled circles only; see text for discussion) and the calibration equation of *Prahl et al.* [1988] (thin solid line) and *Müller et al.* [1998] (thin dashed line). The dashed thick line is the regression of the minimal data set (see text for discussion) for maSSTs above 24°C only. Data include $U^{K'}_{37}$ values reported previously by other investigators (see Table 1). (b) Same as Figure 1a but for maSSTs above 24°C only. The three labeled core top samples are excluded in the minimal data set (see text for discussion).

generally restricted to the warm pool north of the equator, and lower values in the cold tongue off Peru (Figures 2a and 2b). The $U^{K'}_{37}$ values are statistically significantly correlated with maSST ($U^{K'}_{37}$ = (0.027 ± 0.003) maSST + (0.207 ± 0.062); r^2 = 0.78, $p < 0.01$), with a root mean square error (RMSE) of 0.044, equivalent to 1.6°C. This regional regression is not statistically different at the 95% confidence level from the culture-derived regression by *Prahl et al.* [1988] or from previous linear global calibrations by *Müller et al.* [1998] and *Conte et al.* [2006], and RMSE only increases to 0.051, 0.053, or 0.058, or ca. 1.8°C, when applying these widely used regressions to the data set from the EEP presented here. Because of the strong correlation between maSSTs and both temperatures at 20 m depth and SSTs in boreal summer, the correlation decreases only slightly when regressing $U^{K'}_{37}$ versus these temperatures

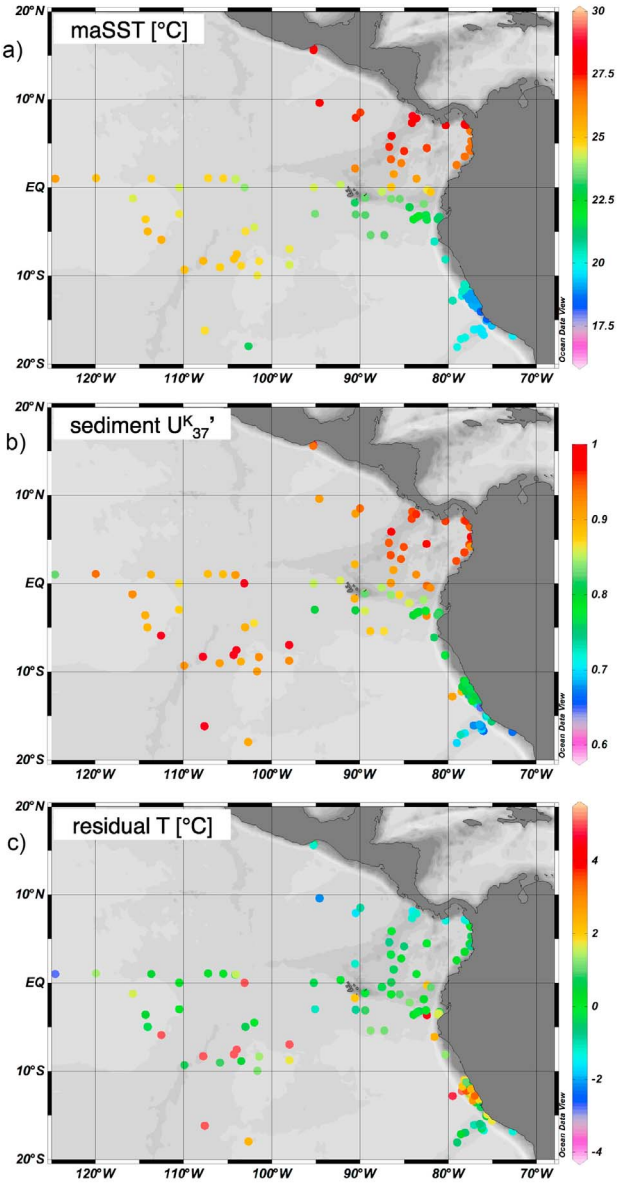

Figure 2. (a) WOA09 mean annual SSTs at the sampling sites, compared to (b) the surface sediment $U^{K'}_{37}$ in the EEP. (c) Residuals are calculated as the difference between $U^{K'}_{37}$ SST estimates (using the calibration of *Prahl et al.* [1988]) and WOA SSTs. Note that the dark red samples west of 95°W in Figures 2b and 2c have a nominal $U^{K'}_{37}$ of 1 due to undetectable triunsatured alkenones (see text for discussion).

Table 2. Summary of Linear Regressions[a]

	a	b	r^2	RMSE
		Full Data Set		
maSST	0.027 ± 0.003	0.207 ± 0.062	0.78	0.044
20 m	0.024 ± 0.002	0.326 ± 0.053	0.76	0.046
50 m	0.024 ± 0.005	0.396 ± 0.088	0.47	0.068
100 m	0.016 ± 0.009	0.612 ± 0.009	0.1	0.086
SST Jan–Mar	0.044 ± 0.006	−0.251 ± 0.160	0.62	0.057
SST Jul–Sep	0.020 ± 0.002	0.403 ± 0.05	0.74	0.047
		Reduced Data Set		
maSST	0.031 ± 0.003	0.110 ± 0.065	0.88	0.033
		Coastal Peru Samples Only		
maSST	0.046 ± 0.021	−0.142 ± 0.420	0.37	0.055
20 m	0.042 ± 0.015	0.011 ± 0.260	0.51	0.048
50 m	0.068 ± 0.022	−0.310 ± 0.349	0.55	0.047
100 m	0.006 ± 0.012	0.847 ± 0.165	0.03	0.059
SST Jan–Mar	0.034 ± 0.033	−0.016 ± 0.751	0.14	0.065
SST Jul–Sep	0.032 ± 0.022	0.210 ± 0.388	0.23	0.062

[a]The variables a and b denote the slope and y-intercept, respectively, of the equation $U^{K'}_{37}$ = a × temperature + b.

(Table 2). For deeper subsurface temperatures (50 and 100 m) and boreal winter SSTs, however, the correlation decreases significantly (Table 2).

[18] Despite the overall good correlation between $U^{K'}_{37}$ and maSST, there are two groups of samples that deviate most notably as evident by their large 'residual' in Figure 2c (see also Figure 1): (1) samples with low alkenone concentrations and (2) samples from the coastal areas off Peru. The residuals, defined as the difference between temperatures estimated from alkenone unsaturation and observed (WOA09) maSSTs, are calculated using the widely applied calibration of *Prahl et al.* [1988] for consistency with previous studies [e.g., *Prahl et al.*, 2010], and because the regional regression above is not statistically different from this culture-derived one. The two groups of samples with notably large residuals will be discussed separately in the following, and eliminated in the analysis and discussion of the 'reduced data set' below.

4.2. Concentration Threshold

[19] Offshore samples that deviate prominently from the correlation with maSST established above are generally characterized by low concentrations of alkenones (note that concentration data are only available for ca. two thirds of the samples). Indeed, all samples, except one, with alkenone concentrations below 50 ng/g have positive residuals, i.e., are biased toward warm SST estimation by 0.3 to 4.4°C (Figure 3). This warm bias is consistent with chromatographic aliasing toward warmer apparent T near the detection limit of the triansaturated alkenone, as discussed by *Grimalt et al.* [2001]. Of these low-concentration samples, 7 samples from the offshore region between 98–112°W and 0–16°S have a nominal $U^{K'}_{37}$ of 1 (dark red dots in Figures 2b and 2c) because the C37:3 is below detection. Taken at face value, these samples appear to overestimate ambient SSTs by 2.8–4.4°C. In following with the recommendation of *Pelejero and Calvo* [2003], however, these latter samples are not included in the data analysis and interpretation here.

[20] The fact that alkenone concentrations are not tightly correlated with $U^{K'}_{37}$ or residuals (Figure 3), even at low concentrations, however, implies that there is no unambiguous way to establish a threshold concentration below which $U^{K'}_{37}$ estimates become unreliable, or uncertainties increase beyond the RMSE of the regression. Rather, SST estimates from sites with alkenone concentrations below 50–100 ng/g should generally be interpreted with caution. This concentration threshold is in line with previous recommendations [*Villanueva and Grimalt*, 1996]. For the 'reduced data set' below, we thus eliminate all samples with concentrations below 100 ng/g (n = 12) or very low peak areas for samples where concentrations were not quantified due to lack of an internal standard (n = 4).

4.3. Coastal Peru

[21] *Prahl et al.* [2010] noted that alkenone samples from the upwelling zone off Peru are characterized by a consistent positive residual, i.e., are biased toward warm SST estimation by 2.1 ± 0.7°C. Fifteen additional samples from this region presented here corroborate this observation. Taken together, 22 samples from the upwelling maximum between 11–15°S and 76–79°W are thus biased toward warm SSTs, 17 even beyond the RMSE of 1.6°C, whereas only 3 samples show a negative residual. Similarly, nearshore samples to the north of this region of maximum upwelling are also biased toward warmer SSTs (Figure 2c). The region of warm skewing is bounded to the south by a transect of samples perpendicular to the coast, which do not exhibit any residual beyond the RMSE [*Calvo et al.*, 2001; *Prahl et al.*, 2006; this study]. The warm-biased samples at 3–4°S/81°W are juxtaposed with sites further offshore that do not show this warm bias, but a lack of samples does not permit to constrain the offshore extent of the anomalous $U^{K'}_{37}$ SST estimates off Peru further south. Because of the strong seasonality in

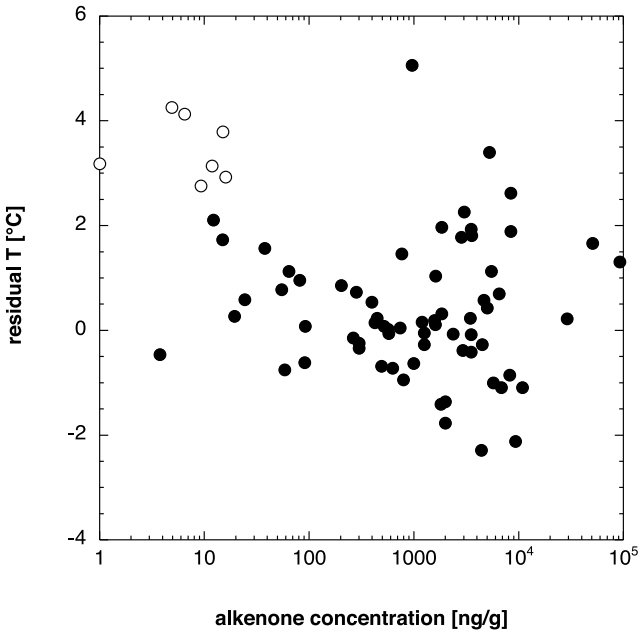

Figure 3. Residual temperatures versus alkenone concentration (note the logarithmic scale on the x axis; note also that concentration data are not available for all samples). The open symbols indicate samples that are characterized by a nominal $U^{K'}_{37}$ of 1 (see text for discussion).

hydrography and biological production in this region, it is conceivable that alkenone unsaturation is skewed toward seasonal or even sub-surface temperatures. However, this inference is not borne out by regressions of the coastal Peru $U^{K'}_{37}$ data versus winter or summer temperatures, or versus subsurface temperatures, which show poor correlations (Table 2).

[22] Viewed in the context with results from the Gulf of Alaska and other sites along the eastern Pacific margin, *Prahl et al.* [2010] argued that the distribution of positive residuals is consistent with a systematic summer skewing of alkenone SST estimates, driven by seasonal production during the non-upwelling, low-nutrient season. In the context of the EEP data presented here, however, the anomalously warm $U^{K'}_{37}$ SST estimates off Peru are more difficult to explain, not least due to the coincidence of warm SSTs with maximum diatom production (see above). Thus, whereas all the warm-biased samples off Peru are characterized by a strong seasonality in surface ocean temperatures, residuals are not generally correlated with seasonality in the EEP ($r^2 = 0.11$). The Peru upwelling is not only characterized by strong seasonality in SSTs but also by high nutrient (phosphate) concentrations in surface waters, and, following the reasoning by *Prahl et al.* [2010], one might expect a correlation between phosphate concentrations and T residuals. However, phosphate concentrations in surface waters are an equally poor predictor of T residuals in the EEP ($r^2 = 0.17$). Finally, the samples from the Peru upwelling do not stand out in terms of their overall alkenone/alkenoate signature either, compared to samples with low residual. Thus, %K37, %K38 and ME/K37 are within the same ranges (49–61%, 33–49%, and 0–0.1, respectively), irrespective of the samples' deviation from the regional or global regression. These alkenone/alkenoate signatures are also within the range of values reported by *Prahl et al.* [2006] for multicore samples off the west coast of South America. In summary, it thus appears that while samples from the near-coastal upwelling center off Peru stand out markedly in terms of their alkenone unsaturation, there is no a priori means of identifying these samples from the biophysical setting or the sedimentary record, respectively.

[23] We note that *Schneider et al.* [1996] observed a similar 'warm' offset between alkenone T estimates and modern maSST data in the inner coastal upwelling centers off Namibia. Whereas it is conceivable that physiological or biogeographic factors control the biased T estimates in both these regions of intense seasonal upwelling, it is possibly also the poorly constrained modern surface ocean temperature near the coast that causes $U^{K'}_{37}$ values to deviate markedly from the global regression. For instance, AVHRR satellite measurements (http://geology.usgs.gov/peter/ocean.shtml) indicate annual average SSTs off Peru up to 2.5°C warmer compared to the WOA data for the same sites, which would account for most of the offset between $U^{K'}_{37}$ SST estimates and maSSTs. In addition, WOA does not capture such strong small-scale SST variability as presented by *Gutiérrez et al.* [2011], for example.

[24] An alternative hypothesis to explain the warm bias off Peru was first proposed by *Rein et al.* [2005]. Because of maximum abundances of alkenone synthesizing coccolithophoridae during El Niño warm water anomalies when surface waters are nutrient deplete, the alkenone paleothermometer in this distinctive region preferentially records sea surface conditions during El Niño events. Sediment trap time series in the Gulf of California and the Santa Barbara Basin, for instance, have indeed shown that coccolithophores reach maximum abundances and fluxes during the oligotrophic conditions associated with El Niño events [e.g., *Ziveri and Thunell*, 2000; *De Bernardi et al.*, 2005]. However, until detailed ocean time series stations, including sediment trap time series of alkenone fluxes and composition, are available for the coastal Peru upwelling region, the two non-exclusive scenarios detailed above cannot be resolved.

4.4. Reduced Data Set

[25] Much of the conflicting interpretation of SST records from the EEP (see above) pertains to the offshore environments outside the near-coastal upwelling maximum off Peru. It thus seems justified to analyze and discuss $U^{K'}_{37}$ of a subset of the EEP data presented here, i.e., a reduced data set that excludes samples from 11–15°S and 76–79°W and from around 3°S/81°W. As detailed above, samples with alkenone concentrations below 100 ng/g are also culled from this reduced data set. Compared to the full data set, the correlation between $U^{K'}_{37}$ and maSST for the reduced data set ($n = 76$) increases significantly ($r^2 = 0.88$) and the regression changes to $U^{K'}_{37} = (0.031 \pm 0.003)$ maSST + (0.110 ± 0.065) (Figure 1), which is statistically identical to the culture-derived regression from *Prahl et al.* [1988] and global linear regressions [*Müller et al.*, 1998; *Conte et al.*, 2006] for the range of maSSTs considered here. The RMSE for the regression of the reduced data set decreases to 0.033 (equivalent to ca. 1°C) for the equation derived here, and to 0.034 when using the calibration of *Prahl et al.* [1988].

4.5. Seasonality, Nutrients and Salinity

[26] As detailed above, residual Ts in the EEP are not generally correlated with seasonality or annual average phosphate concentrations in surface waters. Since both nutrient (phosphate) concentrations and salinities have been postulated to affect alkenone unsaturation [*Conte et al.*, 1998; *Harada et al.*, 2003; *Prahl et al.*, 2003; *Rosell-Melé*, 1998], we also performed multivariate regression with both these variables versus $U^{K'}_{37}$. No discernible improvement from including either salinity, phosphate concentrations, or both, in the regression within the range of maSSTs in the EEP is observed. In each case, the r^2 remains at 0.78 for the full data set, and at 0.88 for the reduced data set, respectively. This lack of obvious influences of these variables on $U^{K'}_{37}$, and the absence of evidence for changes in the alkenone/alkenoate signature (see above) corroborate earlier inferences that these factors are generally minor control [*Herbert*, 2003; *Müller et al.*, 1998]. It thus appears that environmental conditions in lab cultures exceed even the significant diversity in environmental conditions encountered in the EEP [see *Herbert*, 2001, 2003].

[27] We also note that, in contrast to residuals from foraminiferal transfer functions [*Feldberg and Mix*, 2002], the geographical distribution of residuals outside the Peru upwelling zone is random, without obvious link to oceanographic or biogeographic features (see Figure 2c). Finally, the residuals are independent of water depth at the sampling site. This provides evidence against significant water column

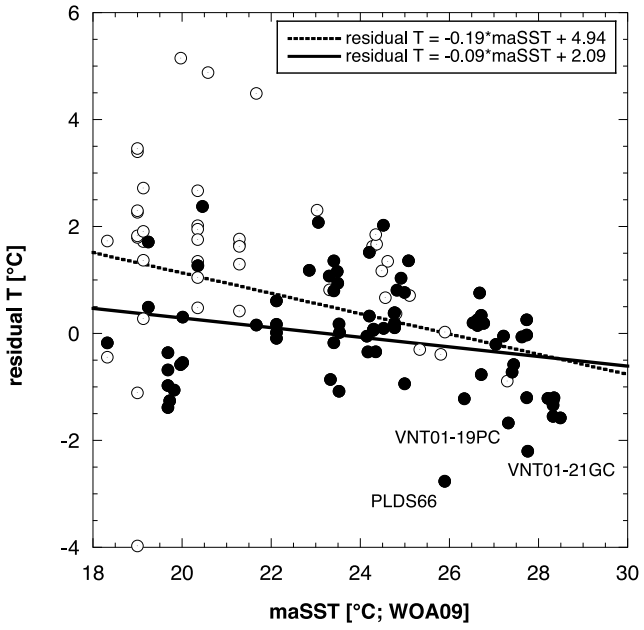

Figure 4. Residual temperatures versus maSSTs (WOA 09). Lines represent the best linear fit for the full (thick dotted line; all data points) and the reduced data sets (thick solid line, filled circles only; see text for discussion). The three core tops with large negative residuals at high maSST are discussed in the text.

modification of the alkenone signal, in contrast to depth dependent carbonate dissolution, which has been shown to affect foraminiferal Mg/Ca in the EEP [*Lea et al.*, 2006; *Mekik et al.*, 2007].

4.6. Residuals Versus maSST and "the Warm End"

[28] As evident from Figure 4, there is a weak negative correlation ($r^2 = 0.17$; $p < 0.01$) of residual temperatures versus maSST for the complete data set over the full range of maSSTs. However, this correlation is largely caused by the two distinct sets of samples with large positive residuals (see above), since the correlation of residuals versus maSST of the reduced data set decreases to $r^2 = 0.06$ ($p < 0.05$; Figure 4). In following with *Sonzogni et al.* [1997], we also explored the correlation of residuals versus maSST for the 'warm end,' adopting the rather arbitrary definition of maSST > 24°C. Above 24°C, the residuals of both the complete and reduced data sets are statistically significantly correlated with maSST ($r^2 = 0.42$ and 0.33, respectively, $p < 0.01$), and the slope of the regression of $U^{K'}_{37}$ versus maSST decreases to 0.012 or 0.021, respectively. The decrease in slope, or the negative correlation between residuals and maSST, is exacerbated, however, by a group of samples with large negative residuals (−1.7 to −2.8) at high maSSTs, all of which derive from piston and gravity core surfaces (Figure 4, see also Figure 1b), which could possibly sample non-late Holocene, colder conditions. Ignoring these three samples, the regression between the $U^{K'}_{37}$ and maSST for the reduced data set above 24°C is $U^{K'}_{37} = 0.024\ maSST + 0.290$ ("minimal" data set regression in Figure 2). This 'warm end' regression is statistically indistinguishable from the regression of all EEP $U^{K'}_{37}$ data versus maSST, and the maximum difference at the warmest end ($U^{K'}_{37} = 0.999$) is 0.1°C. The careful analysis of "warm-end" samples presented here thus suggests that there is no statistically significant flattening of the regression of $U^{K'}_{37}$ versus maSST.

5. Conclusions and Paleoceanographic Implications

[29] The present compilation of $U^{K'}_{37}$ in surface sediments from the EEP shows that alkenone unsaturation outside the near-coastal upwelling zone off Peru conforms with previously established global calibrations of this paleothermometer, with RMSEs of the regression below the accepted uncertainties of $U^{K'}_{37}$ SST estimation. Off Peru, however, alkenone unsaturation at many sites appears to systematically over-estimate maSSTs by up to 4°C. While this coastal zone of maximum upwelling is characterized by strong seasonality and high nutrient concentrations, neither descriptor is a reliable predictor of warm aliasing of $U^{K'}_{37}$ outside this restricted ocean region. We posit that the apparent warm bias is caused either by substantial small-scale SST variability not captured by WOA, or by skewing of the alkenone unsaturation record toward El Niño conditions, as first proposed by *Rein et al.* [2005]. In the absence of detailed time series studies of alkenone unsaturation in the near-coastal upwelling zone off Peru, however, the apparent warm bias of alkenone paleothermometry there remains unexplained.

[30] With respect to the contrasting SST reconstructions reviewed in the introduction, the observations summarized here lead to the following, specific, paleoceanographic implications.

[31] 1. The warm bias of alkenone-derived SST estimates off Peru implies that mean annual SSTs could have been much colder during the glacial period than reflected in the 'summertime' $U^{K'}_{37}$ ratios. This would help reconcile $U^{K'}_{37}$-based reconstructions with foraminiferal transfer function estimates [*Feldberg and Mix*, 2002, 2003], which suggest a glacial cooling of ~10°C slightly outside and to the south of the coastal upwelling area (16°S, 76–77°W). Since the warm bias of the $U^{K'}_{37}$ estimates is limited to the nearshore areas, however, the discrepancy between both estimates beyond the near-coastal upwelling maximum remains unresolved.

[32] 2. Based on the compilation of 17 $U^{K'}_{37}$ records from the EEP, *Dubois et al.* [2009] concluded that the EEP cold tongue south of the equator intensified during the LGM. Given that the data presented here do not display any systematic seasonal, salinity, nutrient, or 'warm-end' bias of the $U^{K'}_{37}$ paleothermometer outside of the near-coastal upwelling maximum this seems the more plausible scenario compared to a weakening of the cold tongue deduced from planktonic foraminiferal $\delta^{18}O$ [*Koutavas and Lynch-Stieglitz*, 2003], a proxy which has been shown to be also affected by sea surface salinities in the EEP [*Rincón-Martínez et al.*, 2011].

[33] **Acknowledgments.** This study would not have been possible without the generosity and efforts of a number of individuals who kindly and generously shared sample material, data, and expertise. The authors are especially indebted to B. Conard (Deep-Sea Sample Repository at Oregon State University), M. Conte, T. Eglinton, D. Gutiérrez, L. Keigwin, S. Kusch, R. Lotti (Deep-Sea Sample Repository at Lamont-Doherty Earth Observatory), F. Mekik, and G. Mollenhauer. The authors are grateful to Carles Pelejero and two anonymous colleagues for constructive and

thoughtful reviews of an earlier version of this paper. Funding of this study was provided by NSERC Canada, NSF (OCE0850143, OCE1003387, OCE0648164), and the Canadian Institute for Advanced Research (CIFAR).

References

Aksnes, D. L., et al. (1994), Representation of Emiliania huxleyi in phytoplankton simulation models: A first approach, *Sarsia*, *79*(4), 291–300.

Antonov, J. I., et al. (2010) *World Ocean Atlas 2009*, vol. 2, *Salinity*, *NOAA Atlas NESDIS*, vol. 69, edited by S. Levitus, 184 pp., NOAA, Silver Spring, Md.

Arntz, W., and E. Fahrbach (1991), *El Nino–Klimaexperiment der Natur*, 263 pp., Springer, New York.

Bakun, A. (1987), Monthly variability in the ocean habitat off Peru as deduced from maritime observations, 1953 to 1984, in *Peruvian Anchoveta and its Upwelling Ecosystem*, edited by D. Pauly and I. Tsukayama, pp. 46–74, Inst. del Mar del Peru, Callao.

Bakun, A., and C. S. Nelson (1991), The seasonal cycle of wind stress curl in sub-tropical boundary current regions, *J. Phys. Oceanogr.*, *21*, 1815–1834, doi:10.1175/1520-0485(1991)021<1815:TSCOWS>2.0.CO;2.

Barber, R. T., and F. P. Chavez (1983), Biological consequences of El Nino, *Science*, *222*, 1203–1210, doi:10.1126/science.222.4629.1203.

Barber, R. T., and F. P. Chavez (1986), Ocean variability in relation to living resources during the 1982/83 El Nino, *Nature*, *319*, 279–285, doi:10.1038/319279a0.

Brassell, S. C. (1993), Applications of biomarkers for delineating marine paleoclimatic fluctuations during the Pleistocene, in *Organic Geochemistry: Principles and Applications*, *Topics Geobiol.*, vol. 11, edited by M. H. Engel and S. A. Macko, pp. 699–738, Plenum, New York.

Bruland, K. W., E. A. Rue, G. J. Smith, and G. R. DiTullio (2005), Iron, macronutrients and diatom blooms in the Peru upwelling regime: Brown and blue waters of Peru, *Mar. Chem.*, *93*, 81–103, doi:10.1016/j.marchem.2004.06.011.

Calvo, E., et al. (2001), Insolation dependence of the southeastern Subtropical Pacific sea surface temperature over the last 400 kyrs, *Geophys. Res. Lett.*, *28*(12), 2481–2484, doi:10.1029/2000GL012024.

Chavez, F. P. (1989), Size distribution of phytoplankton in the central and eastern tropical Pacific, *Global Biogeochem. Cycles*, *3*, 27–35, doi:10.1029/GB003i001p00027.

Chavez, F. P. (1995), A comparison of ship and satellite chlorophyll from California and Peru, *J. Geophys. Res.*, *100*, 24,855–24,862, doi:10.1029/95JC02738.

Chavez, F. P. (2005), Biological consequences of interannual to multidecadal variability, in *The Sea*, vol. 13, edited by A. Robinson and K. Brink, pp. 643–679, Harvard Univ. Press, Cambridge, Mass.

Chavez, F. P., K. R. Buck, K. H. Coale, J. H. Martin, G. R. DiTullio, N. A. Welschmeyer, A. C. Jacobson, and R. T. Barber (1991), Growth rates, grazing, sinking, and iron limitation of equatorial Pacific phytoplankton, *Limnol. Oceanogr.*, *36*, 1816–1833, doi:10.4319/lo.1991.36.8.1816.

Chavez, F. P., K. R. Buck, S. K. Service, J. Newton, and R. T. Barber (1996), Phytoplankton variability in the central and eastern tropical Pacific, *Deep Sea Res., Part II*, *43*, 835–870, doi:10.1016/0967-0645(96)00028-8.

Chavez, F. P., A. Bertrand, R. Guevara, P. Soler, and J. Csirke (2008), The northern Humboldt Current System: Brief history, present status and a view towards the future, *Prog. Oceanogr.*, *79*(2–4), 95–105, doi:10.1016/j.pocean.2008.10.012.

Conte, M. H., et al. (1998), Genetic and physiological influences on the alkenone/alkenoate versus growth temperature relationship in Emiliania huxleyi and Gephyrocapsa oceanica, *Geochim. Cosmochim. Acta*, *62*, 51–68, doi:10.1016/S0016-7037(97)00327-X.

Conte, M. H., et al. (2006), Global temperature calibration of the alkenone unsaturation index in surface waters and comparison with surface sediments, *Geochem. Geophys. Geosyst.*, *7*, Q02005, doi:10.1029/2005GC001054.

De Bernardi, B., et al. (2005), Coccolithophore export production during the 1997–1998 El Niño event in Santa Barbara Basin (California), *Mar. Micropaleontol.*, *55*, 107–125, doi:10.1016/j.marmicro.2005.02.003.

DiTullio, G., M. E. Geesey, J. M. Maucher, M. B. Alm, S. F. Riseman, and K. W. Bruland (2005), Influence of iron on algal community composition and physiological status in the Peru upwelling system, *Limnol. Oceanogr.*, *50*, 1887–1907, doi:10.4319/lo.2005.50.6.1887.

Dubois, N., M. Kienast, C. Normandeau, and T. D. Herbert (2009), Eastern equatorial Pacific cold tongue during the Last Glacial Maximum as seen from alkenone paleothermometry, *Paleoceanography*, *24*, PA4207, doi:10.1029/2009PA001781.

Dubois, N., et al. (2011), Millennial-scale variations in hydrography and biogeochemistry in the Eastern Equatorial Pacific over the last 100 kyr, *Quat. Sci. Rev.*, *30*(1–2), 210–223, doi:10.1016/j.quascirev.2010.10.012.

Echevin, V., O. Aumont, J. Ledesma, and G. Flores (2008), The seasonal cycle of surface chlorophyll in the Peruvian upwelling system: A modelling study, *Prog. Oceanogr.*, *79*, 167–176, doi:10.1016/j.pocean.2008.10.026.

Feldberg, M. J., and A. C. Mix (2002), Sea-surface temperature estimates in the Southeast Pacific based on planktonic foraminiferal species; modern calibration and Last Glacial Maximum, *Mar. Micropaleontol.*, *44*(1–2), 1–29, doi:10.1016/S0377-8398(01)00035-4.

Feldberg, M. J., and A. C. Mix (2003), Planktonic foraminifera, sea surface temperatures, and mechanisms of oceanic change in the Peru and south equatorial currents, 0–150 ka BP, *Paleoceanography*, *18*(1), 1016, doi:10.1029/2001PA000740.

Fiedler, P. C. (2002), Environmental change in the eastern tropical Pacific Ocean: Review of ENSO and decadal variability, *Mar. Ecol. Prog. Ser.*, *244*, 265–283, doi:10.3354/meps244265.

Friederich, G. E., J. Ledesma, O. Ulloa, and F. P. Chavez (2008), Air–sea carbon dioxide fluxes in the coastal southeastern tropical Pacific, *Prog. Oceanogr.*, *79*(2–4), 156–166, doi:10.1016/j.pocean.2008.10.001.

Garcia, H. E., et al. (2010), *World Ocean Atlas 2009*, vol. 4, *Nutrients*, *NOAA Atlas NESDIS*, vol. 71, edited by S. Levitus, 398 pp., NOAA, Silver Spring, Md.

Grimalt, J. O., et al. (2001), Sea surface paleotemperature errors in U-37(K′) estimation due to alkenone measurements near the limit of detection, *Paleoceanography*, *16*, 226–232, doi:10.1029/1999PA000440.

Gutiérrez, D., et al. (2011), Coastal cooling and increased productivity in the main upwelling zone off Peru since the mid-twentieth century, *Geophys. Res. Lett.*, *38*, L07603, doi:10.1029/2010GL046324.

Harada, N., et al. (2003), Characteristics of alkenones synthesized by a bloom of Emiliania huxleyi in the Bering Sea, *Geochim. Cosmochim. Acta*, *67*, 1507–1519, doi:10.1016/S0016-7037(02)01318-2.

Haug, G. H., et al. (2005), North Pacific seasonality and the glaciation of North America 2.7 million years ago, *Nature*, *433*(7028), 821–825, doi:10.1038/nature03332.

Herbert, T. D. (2001), Review of alkenone calibrations (culture, water column, and sediments), *Geochem. Geophys. Geosyst.*, *2*(2), 1005, doi:10.1029/2000GC000055.

Herbert, T. D. (2003), Alkenone paleotemperature determinations, in *Treatise on Geochemistry*, vol. 6, *The Oceans and Marine Geochemistry*, edited by H. D. Holland and K. K. Turekian, pp. 391–432, Elsevier, Amsterdam, doi:10.1016/B0-08-043751-6/06115-6.

Horikawa, K., et al. (2006), Spatial and temporal sea-surface temperatures in the eastern equatorial Pacific over the past 150 kyr, *Geophys. Res. Lett.*, *33*, L13605, doi:10.1029/2006GL025948.

Hutchins, D. A., et al. (2002), Phytoplankton iron limitation in the Humboldt Current and Peru Upwelling, *Limnol. Oceanogr.*, *47*, 997–1011, doi:10.4319/lo.2002.47.4.0997.

Iriarte, J. L., and H. E. Gonzalez (2004), Phytoplankton size structure during and after the 1997/1998 El Nino in coastal upwelling area of the northern Humboldt Current System, *Mar. Ecol. Prog. Ser.*, *269*, 83–90, doi:10.3354/meps269083.

Kienast, M., et al. (2006), Eastern Pacific cooling and Atlantic overturning circulation during the last deglaciation, *Nature*, *443*, 846–849, doi:10.1038/nature05222.

Koutavas, A., and J. Lynch-Stieglitz (2003), Glacial-interglacial dynamics of the eastern equatorial Pacific cold tongue-Intertropical Convergence Zone system reconstructed from oxygen isotope records, *Paleoceanography*, *18*(4), 1089, doi:10.1029/2003PA000894.

Koutavas, A., and J. P. Sachs (2008), Northern timing of deglaciation in the eastern equatorial Pacific from alkenone paleothermometry, *Paleoceanography*, *23*, PA4205, doi:10.1029/2008PA001593.

Kusch, S., et al. (2010), Timescales of lateral sediment transport in the Panama Basin as revealed by radiocarbon ages of alkenones, total organic carbon and foraminifera, *Earth Planet. Sci. Lett.*, *290*, 340–350, doi:10.1016/j.epsl.2009.12.030.

Landry, M. R., and D. L. Kirchman (2002), Microbial community structure and variability in the tropical Pacific, *Deep Sea Res., Part II*, *49*, 2669–2693, doi:10.1016/S0967-0645(02)00053-X.

Lea, D. W., et al. (2006), Paleoclimate history of the Galápagos surface waters over the last 135 000 yr, *Quat. Sci. Rev.*, *25*, 1152–1167, doi:10.1016/j.quascirev.2005.11.010.

Leduc, G., et al. (2007), Moisture transport across Central America as a positive feedback on abrupt climatic changes, *Nature*, *445*, 908–911, doi:10.1038/nature05578.

Leduc, G., et al. (2010), Holocene and Eemian sea surface temperature trends as revealed by alkenone and Mg/Ca paleothermometry, *Quat. Sci. Rev.*, *29*, 989–1004, doi:10.1016/j.quascirev.2010.01.004.

Li, T., and S. G. H. Philander (1996), On the annual cycle of the eastern equatorial Pacific, *J. Clim.*, *9*, 2986–2998, doi:10.1175/1520-0442(1996)009<2986:OTACOT>2.0.CO;2.

Liu, Z., and T. D. Herbert (2004), High-latitude influence on the eastern equatorial Pacific climate in the early Pleistocene epoch, *Nature*, *427*, 720–723, doi:10.1038/nature02338.

Locarnini, R. A., et al. (2010), *World Ocean Atlas 2009*, vol. 1, *Temperature*, *NOAA Atlas NESDIS*, vol. 68, edited by S. Levitus, 184 pp., NOAA, Silver Spring, Md.

Mekik, F., et al. (2007), A novel approach to dissolution correction of Mg/Ca–based paleothermometry in the tropical Pacific, *Paleoceanography*, *22*, PA3217, doi:10.1029/2007PA001504.

Minas, H. J., and M. Minas (1992), Net community production in high nutrient–low chlorophyll waters of the tropical and Antarctic oceans: Grazing vs iron hypothesis, *Oceanol. . Acta*, *15*, 145–162.

Mitchell, T. P., and J. M. Wallace (1992), The annual cycle in equatorial convection and sea surface temperature, *J. Clim.*, *5*, 1140–1156, doi:10.1175/1520-0442(1992)005<1140:TACIEC>2.0.CO;2.

Mix, A., et al. (1999), Foraminiferal faunal estimates of paleotemperature: Circumventing the no-analog problem yields cool ice age tropics, *Paleoceanography*, *14*(3), 350–359, doi:10.1029/1999PA900012.

Morales, C. E., S. E. Hormazabal, and J. L. Blanco (1999), Interannual variabllity in the mesoscale distribution of the depth of the upper boundary of the oxygen minimum layer off northern Chile (18–24S), *J. Mar. Res.*, *57*, 909–932, doi:10.1357/002224099321514097.

Müller, P. J., and G. Fischer (2003), C37-alkenones as paleotemperature tool: Fundamentals based on sediment traps and surface sedimetns from the South Atlantic Ocean, in *The South Atlantic in the Late Quaternary: Reconstruction of Material Budgets and Current Systems*, edited by G. Wefer et al., pp. 167–193, Springer, Berlin.

Müller, P. J., et al. (1998), Calibration of the alkenone paleotemperature index $U^{K'}_{37}$ based on core-tops from the eastern South Atlantic and the global ocean (60°N–60°S), *Geochim. Cosmochim. Acta*, *62*, 1757–1772, doi:10.1016/S0016-7037(98)00097-0.

Pahnke, K., et al. (2007), Eastern tropical Pacific hydrologic changes during the past 27,000 years from D/H ratios in alkenones, *Paleoceanography*, *22*, PA4214, doi:10.1029/2007PA001468.

Pelejero, C., and E. Calvo (2003), The upper end of the $U^{K'}_{37}$ temperature calibration revisited, *Geochem. Geophys. Geosyst.*, *4*(2), 1014, doi:10.1029/2002GC000431.

Pelejero, C., and J. O. Grimalt (1997), The correlation between the $U^{K'}_{37}$ index and sea surface temperatures in the warm boundary: The South China Sea, *Geochim. Cosmochim. Acta*, *61*(22), 4789–4797, doi:10.1016/S0016-7037(97)00280-9.

Pennington, J. T., K. L. Mahoney, V. S. Kuwahara, D. D. Kobler, R. Calienes, and F. P. Chavez (2006), Primary production in the eastern tropical Pacific: A review, *Prog. Oceanogr.*, *69*, 285–317, doi:10.1016/j.pocean.2006.03.012.

Pisias, N. G., and A. Mix (1997), Spatial and temporal oceanographic variability of the eastern equatorial Pacific during the late Pleistocene: Evidence from Radiolaria microfossils, *Paleoceanography*, *12*(3), 381–393, doi:10.1029/97PA00583.

Prahl, F. G., and S. G. Wakeham (1987), Calibration of unsaturation patterns in long-chain ketone compositions for paleotemperature assessment, *Nature*, *330*, 367–369, doi:10.1038/330367a0.

Prahl, F. G., et al. (1988), Further evaluation of long-chain alkenones as indicators of paleoceanographic conditions, *Geochim. Cosmochim. Acta*, *52*(9), 2303–2310, doi:10.1016/0016-7037(88)90132-9.

Prahl, F. G., M. A. Sparrow, and G. V. Wolfe (2003), Physiological impacts on alkenone paleothermometry, *Paleoceanography*, *18*(2), 1025, doi:10.1029/2002PA000803.

Prahl, F. G., et al. (2006), Alkenone paleothermometry: Biological lessons from marine sediment records off western South America, *Geochim. Cosmochim. Acta*, *70*(1), 101–117, doi:10.1016/j.gca.2005.08.023.

Prahl, F. G., et al. (2010), Systematic pattern in $U^{K'}_{37}$ – Temperature residuals for surface sediments from high latitude and other oceanographic settings, *Geochim. Cosmochim. Acta*, *74*(1), 131–143, doi:10.1016/j.gca.2009.09.027.

Rein, B., A. Lückge, L. Reinhardt, F. Sirocko, A. Wolf, and W.-C. Dullo (2005), El Niño variability off Peru during the last 20,000 years, *Paleoceanography*, *20*, PA4003, doi:10.1029/2004PA001099.

Rincón-Martínez, D., et al. (2011), Tracking the equatorial front in the eastern equatorial Pacific Ocean by the isotopic and faunal composition of planktonic foraminifera, *Mar. Micropaleontol.*, *79*, 24–40, doi:10.1016/j.marmicro.2011.01.001.

Rojas de Mendiola, B. (1981), Seasonal phytoplankton distribution along the Peruvian coast, in *Coastal Upwelling*, *Coastal Estuarine Sci.*, vol. 1, edited by F. A. Richards, pp. 348–356, AGU, Washington, D. C., doi:10.1029/CO001p0348.

Rosell-Melé, A. (1998), Interhemispheric appraisal of the value of alkenone indices as temperature and salinity proxies in high-latitude locations, *Paleoceanography*, *13*, 694–703, doi:10.1029/98PA02355.

Rosell-Melé, A., et al. (2001), Precision of the current methods to measure the alkenone proxy $U^{K'}_{37}$ and absolute alkenone abundance in sediments: Results of an interlaboratory comparison study, *Geochem. Geophys. Geosyst.*, *2*(7), 1046, doi:10.1029/2000GC000141.

Scheidegger, K. F., and L. A. Krissek (1981), Zooplankton and nekton: Natural barriers to the seaward transport of suspended terrigenous particles off Peru, in *Responses of the Sedimentary Regime to Present Coastal Upwelling*, edited by E. Suess and J. Thiede, pp. 303–336, Plenum, New York.

Schneider, R. R., et al. (1995), Late Quaternary surface circulation in the east equatorial South Atlantic: Evidence form alkenone sea surface temperatures, *Paleoceanography*, *10*, 197–219, doi:10.1029/94PA03308.

Schneider, R., et al. (1996), Late Quaternary surface temperatures and productivity in the east-equatorial South Atlantic: Response to changes in trade/monsoon wind forcing and surface water advection, in *The South Atlantic: Present and Past Circulation*, edited by G. Wefer et al., pp. 527–551, Springer, Berlin.

Schneider, B., et al. (2010), Disentangling seasonal signals in Holocene climate trends by satellite-model-proxy integration, *Paleoceanography*, *25*, PA4217, doi:10.1029/2009PA001893.

Sonzogni, C., et al. (1997), Temperature and salinity effects on alkenone ratios measured in surface sediments from the Indian Ocean, *Quat. Res.*, *47*, 344–355, doi:10.1006/qres.1997.1885.

Steinke, S., et al. (2008), Proxy dependence of the temporal pattern of deglacial warming in the tropical South China Sea: Toward resolving seasonality, *Quat. Sci. Rev.*, *27*, 688–700, doi:10.1016/j.quascirev.2007.12.003.

Strickland, J. D. H., R. W. Eppley, and B. Rojas de Mendiola (1969), Phytoplankton populations, nutrients and photosynthesis in Peruvian coastal waters, *Bol. Inst. Mar Peru*, *2*, 37–45.

Toggweiler, J. R., K. Dixon, and W. S. Broecker (1991), The Peru Upwelling and the Ventilation of the South Pacific Thermocline, *J. Geophys. Res.*, *96*(C11), 20,467–20,497, doi:10.1029/91JC02063.

Tyrrell, T., and A. Merico (2004), *Emiliania huxleyi: Bloom observations and the conditions that induce them*, in *Coccolithophores: From Molecular Processes to Global Impact*, edited by H. R. Thierstein and J. R. Young, pp. 75–97, Springer, Berlin.

Villanueva, J., and J. O. Grimalt (1996), Pitfalls in the chromatographic determination of the alkenone $U^{K'}_{37}$ index for paleotemperature estimation, *J. Chromatogr. A*, *723*, 285–291, doi:10.1016/0021-9673(95)00471-8.

Wilkerson, F. P., R. C. Dugdale, R. M. Kudela, and F. P. Chavez (2000), Biomass and productivity in Monterey bay, California: Contribution of the large phytoplankton, *Deep Sea Res.*, *47*, 1003–1022, doi:10.1016/S0967-0645(99)00134-4.

Wyrtki, K. (1981), An estimate of equatorial upwelling in the Pacific, *J. Phys. Oceanogr.*, *11*, 1205–1214, doi:10.1175/1520-0485(1981)011<1205:AEOEUI>2.0.CO;2.

Xie, S.-P., H. Xu, W. S. Kessler, and M. Nonaka (2005), Air–sea interaction over the Eastern Pacific Warm Pool: Gap winds, thermocline dome, and atmospheric convection, *J. Clim.*, *18*, 5–20, doi:10.1175/JCLI-3249.1.

Ziveri, P., and R. C. Thunell (2000), Coccolithophore export production in Guayamas Basin, Gulf of California: Response to climate forcing, *Deep Sea Res., Part II*, *47*, 2073–2100, doi:10.1016/S0967-0645(00)00017-5.

C. Chazen and T. D. Herbert, Department of Geological Sciences, Brown University, 324 Brook St., Box 1846, Providence, RI 02912, USA.

N. Dubois, School of Earth, Atmospheric and Environmental Sciences, University of Manchester, Oxford Road, Manchester M13 9PL, UK.

S. Higginson, M. Kienast, G. MacIntyre, and C. Normandeau, Department of Oceanography, Dalhousie University, 1355 Oxford St., Halifax, NS B3H 4R2, Canada. (markus.kienast@dal.ca)